

Received September 13, 2018, accepted October 8, 2018, date of publication October 22, 2018, date of current version November 14, 2018.

Digital Object Identifier 10.1109/ACCESS.2018.2877039

Electrical Tree Initiation Properties in Cross-Linked Polyethylene Under DC-Impulse Composite Voltages

HECHEN LIU¹, YANDA LI¹, YUNPENG LIU^{1,2}, MINGJIA ZHANG¹,
XIAOBIN XU¹, AND AIJING LIU¹

¹Hebei Provincial Key Laboratory of Power Transmission Equipment Security Defense, North China Electric Power University, Baoding 071003, China

²State Key Laboratory of Alternate Electrical Power System with Renewable Energy Sources, North China Electric Power University, Beijing 102206, China

Corresponding author: Hechen Liu (hc.liu@ncepu.edu.cn)

This work was supported in part by the Natural Science Foundation of Hebei Province under Grant E2018502133, in part by the National Key Research and Development Program of China under Grant 2016YFB0900705, and in part by the Fundamental Research Funds for the Central Universities under Grant 2018MS079.

ABSTRACT DC cables may be subjected to impulse overvoltage during operation, which may cause electrical tree inside the cable insulation. So, it is necessary to investigate the influence of impulse voltage on the insulation of dc cable. The initiation characteristics of electrical trees in cross-linked polyethylene under dc-impulse composite voltages were investigated in this paper. The influences of pre-stressed dc voltage, impulse voltage, polarity, and space charge accumulation on the initiation characteristics were analysed. The experimental results indicated that the impulse voltage would facilitate the electrical tree initiation and had an obvious polarity effect. Electrical tree initiation voltages under positive impulse voltages were lower than those under negative ones, which was independent of the polarity of the pre-stressed dc voltage. With the increase of the pre-stressed dc voltage, the initiation impulse voltages declined when dc and impulse voltages were of the same polarity. In the presence of opposite polarity, the initiation impulse voltage did not change obviously at first and then increased with the pre-stressed dc voltage.

INDEX TERMS Electrical tree, XLPE, DC-impulse composite, initiation properties, polarity effect.

I. INTRODUCTION

As flexible DC transmission technology and new energy sources are being developed, cross-linked polyethylene (XLPE) HVDC cable has been used widely, owing to its superior insulating properties and low cost [1], [2]; however, some defects may form in XLPE cables during production and operation, such as impurities, small bubbles, embossment of semi-conducting layers, *etc.* [3], [4]. These defects may lead to the accumulation of space charges and local field concentration in the insulation, which may result in electrical tree initiation or even breakdown [5].

Researchers have studied the characteristics of electrical trees under DC voltage in XLPE insulation materials, containing DC trees, DC grounded trees, DC trees with polarity reversal, DC superimposed AC trees, *etc.* [6]–[8]. It was found that space charge accumulated near the needle tip had a significant influence on the initiation and growth characteristics of the DC electrical tree [9]. It was also the main reason for the polarity effect [10], [11]. Besides, temperature [7],

mechanical stress [12], defect type [13], DC pre-stress [14], polarity reversal [15] and magnetic field [16] also influenced the initiation properties of DC electrical tree.

During the operation of DC cables, the insulation may be subjected to transient overvoltage, such as lightning impulse voltage and switching impulse voltage, which may induce electrical trees. Thus, it is necessary to investigate the electrical tree initiation properties in XLPE under DC-impulse voltage. Noto *et al.* [17] studied the initiation properties of LDPE under DC and impulse combined voltages. Fujita *et al.* [18] studied the initiation properties of electrical trees in polymethyl methacrylate (PMMA) with DC superimposed impulse voltages and pointed out that the initiation voltage would increase when DC and impulse voltages were of the same polarity. Ying and Xiaolong [19] investigated the initiation features with pre-stressed DC and impulse voltage, which indicated that the tree initiation ratio increased due to higher impulse voltage, increased DC pre-stress level and shorter rest time between DC pre-stress and impulse voltage.

Chen *et al.* [20] investigated the electrical tree initiation properties of degraded LDPE under DC-impulse voltage. Tao H carried out the tests on the inception and growth characteristics in silicon rubber under combined DC-pulse voltages and found that when the DC voltage increased, the inception pulse voltage with the opposite polarity increased. Besides, the initial tree structure was determined by the pulse voltage polarity [21].

As discussed above, some studies have been conducted on the characteristics of electrical trees under DC-impulse composite voltages in kinds of polymeric materials. However, the influence of pre-stressed DC voltage, impulse voltage, polarity and space charge accumulation on the initiation characteristics of electrical trees should be further investigated, especially in XLPE. In this work, we investigated the initiation characteristics of electrical trees under DC-impulse composite voltages. The pre-stressed DC voltages were set to 0 kV, ± 10 kV, ± 20 kV, ± 30 kV. The impulse voltages were lightning impulse voltage (LI) and switching impulse voltage (SI).

II. EXPERIMENTAL SET-UP

Here, the sample preparation, experimental system, and test methods are introduced.

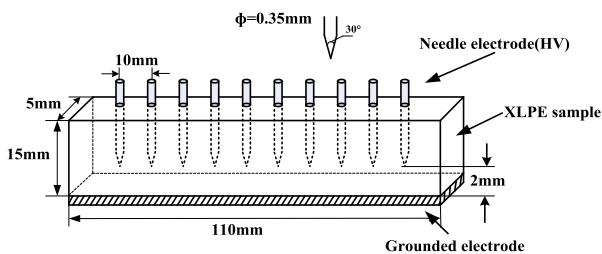


FIGURE 1. Specimen configuration.

A. SAMPLE PREPARATION

A commercially available XLPE WMY4201EHV(YJ-220) material source from Zhejiang Wanma Macromolecule Materials Co., Ltd, was used. First, the XLPE particles were melted and fully cross-linked at 175 °C and 15 MPa for 30 min in a plate vulcanizing press. Afterwards, the sample was cooled to room temperature at a rate of 8 to 9 °C /min by water cooling. The samples were then cut to strip-shape specimens measuring 110 mm \times 5 mm \times 15 mm (Fig.1). Then, the strip-shape specimen was heated to 120 °C, maintained thereat for 10 min until the sample was soft enough for the insertion of ten steel needles, at equal intervals of 10 mm longitudinal spacing. The radius of the steel needle tip was about 6 μ m and the diameter was 0.35 mm. Thereafter, the samples were kept at the elevated temperature for 5 min to eliminate the influence of mechanical stress caused by the insertion of the needle electrodes. Finally, the specimen was cooled at the same rate of 8 to 9 °C /min. To produce a classical needle-plate electrode, a copper foil was affixed to the underneath of sample to form a grounded electrode. In order to reduce the impact of the applied voltage to the

adjacent needle-plate systems, the grounded electrode was separated, thus forming 10 independent needle-plate systems.

B. EXPERIMENTAL SYSTEM AND METHOD

The experimental system is as shown in Fig. 2. The sample was fixed at the bottom of a quartz glass container which was filled with dimethyl silicone oil. On the one hand, the oil could avoid flashover along the surface of the sample; on the other hand, it could fill any uneven surface features to enhance transparency of the sample. The test temperature was adjusted by a temperature controller. To weaken the image shocking caused by electrophoresis under DC voltage, the microscope was placed horizontally. The images of the electrical trees were obtained in real-time from a video microscope which was connected to the computer by a CCD camera. The visual magnification of the microscope was 37.5 \times and the video magnification was 222.5 \times . Initiation of the electrical tree was deemed to be occurred when the tree length reached 10 μ m.

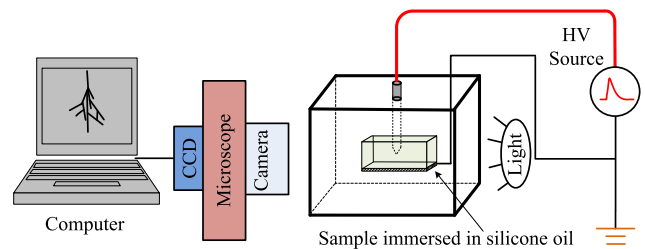


FIGURE 2. Electrical tree experimental and observational system.

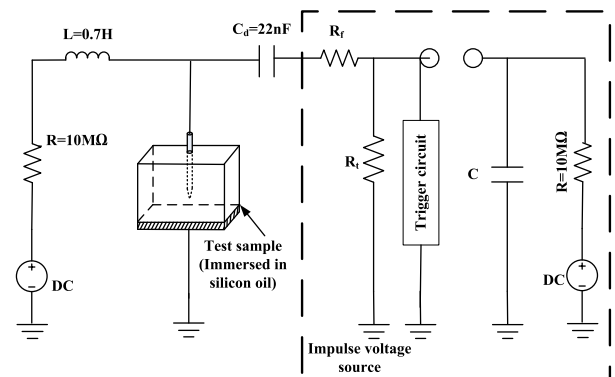


FIGURE 3. The circuit diagram of the experimental system.

The circuit diagram of the experimental system is as shown in Fig.3. In the figure, “R” is the current-limiting resistance which can limit the current when the sample occurs breakdown; “L” is the reactance which can protect the DC voltage source from the harm caused by the impulse voltage; “ C_d ” is the block capacitor which can prevent the DC voltage from entering the impulse voltage generator. The wave front time T_f and wave tail time T_t of LI and SI impulse voltages can be adjusted by wave front resistance R_f , wave tail resistance R_t and main capacitor C. The parameters setting of the impulse voltage generator circuit are as shown in Table 1.

TABLE 1. Parameter setting of the impulse voltage generator circuit.

	$T_1(\mu s)$	$T_2(\mu s)$	$R_1(k\Omega)$	$R_2(k\Omega)$	$C(nF)$
LI	1.2	50	1.4	3.1	22
SI	230	2400	50	15	202

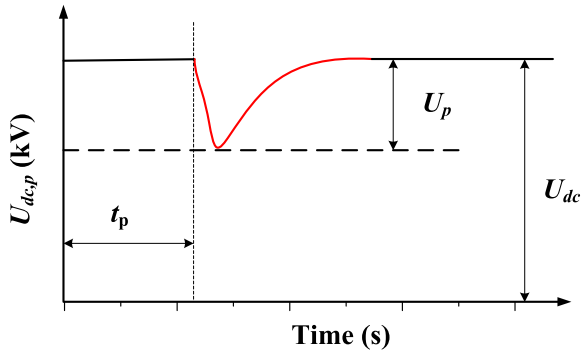


FIGURE 4. The waveform of DC-impulse composite voltages.

During the test, only one needle electrode was tested at a time. First, the pre-stressed DC voltage U_{dc} was increased to a pre-set value at 1 kV/s and maintained for a pre-stressed time (t_p). Here, it was set as 10 s. After that, an impulse voltage U_p was superimposed onto electrode at 2 kV/step until an electrical tree was initiated. Two impulses were applied to the sample at each voltage step and the interval of each impulse was about 60 seconds. After each voltage step, the initiation of the electrical tree was checked. The composite voltage $U_{dc,p}$ was given by Eq. (1) and the waveform of $U_{dc,p}$ was shown in Fig. 4.

$$U_{dc,p} = U_{dc} + U_p \tag{1}$$

U_{dc} were set to 0 kV, ± 10 kV, ± 20 kV, and ± 30 kV. Each type of composite voltages was applied in at least 15 groups of effective tests to obtain a reasonable statistical result. All tests were conducted at room temperature (25 ± 5) °C. DC-impulse voltages of the same polarity were represented as $U_{+dc,+p}$ and $U_{-dc,-p}$; DC-impulse voltages of opposite polarity were represented as $U_{+dc,-p}$ and $U_{-dc,+p}$.

III. EXPERIMENTAL RESULTS

A. ELECTRICAL TREE INITIATION CHARACTERISTICS UNDER LI AND SI VOLTAGES

A Weibull distribution model was used to analyse the electrical tree initiation properties under composite voltages. The model is widely used in reliability analysis and residual service life testing [22], [23]. The probability function of the two-parameter distribution model is given by Eq. (2):

$$F(U) = 1 - \exp\left(-\left[\frac{U}{\alpha}\right]^\beta\right) \tag{2}$$

where, α and β are the scale parameter and configuration parameter, and represent 63.2% of the electrical tree initiation voltage and the range, respectively.

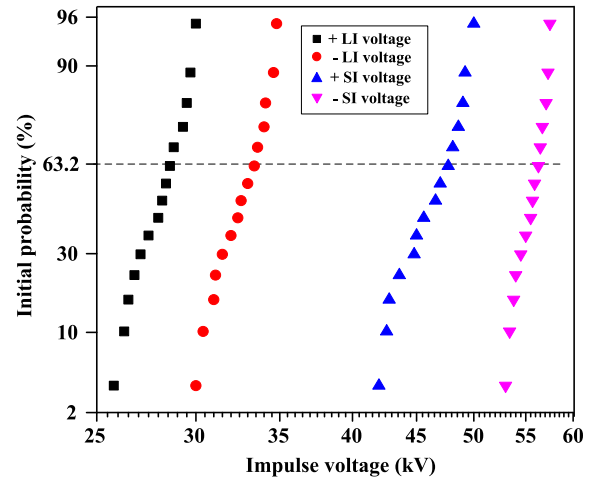


FIGURE 5. Weibull probability graph of electrical tree initiation characteristics under LI and SI voltages.

Fig.5 shows the relationship between initiation probabilities and impulse voltages. It could be seen that the 63.2% LI initiation voltages with positive and negative polarities were 28.7 kV and -33.3 kV, respectively. The 63.2% SI initiation voltages were 47.5 kV and -56.2 kV, respectively. It was found that, although the electrical tree initiation voltage under SI voltage was much larger than that under LI, both of them were much smaller compared to that under pure DC voltage, which was more than ± 70 kV, according to previous researches. When a DC voltage was applied to needle electrode, a homo charge layer formed, which could weaken electrical field strength at the tip of needle and result in a much higher initiation voltage [14]. As for the impulse voltage, the sudden change in voltage would generate significant amounts of electromechanical and thermal energy, which might cause tree initiation at a lower voltage [19]. For an LI voltage, the rising edge was much steeper than that of under SI conditions, which may be why the initiation voltage under LI conditions was smaller than that under SI. Moreover, Fig.5 shows a notable polarity effect on the initiation properties. Specifically, the initiation voltage under positive impulse voltage was lower than that under a negative voltage, for both LI and SI.

B. ELECTRICAL TREE INITIATION CHARACTERS UNDER DC-IMPULSE COMPOSITE VOLTAGES

Fig.6 and Table 2 show the initiation properties of samples under DC-impulse composite voltages. The Y-axis represented the initiation impulse voltage with different U_{dc} pre-stressed. The first and third quadrants showed the results when the polarities of U_{dc} and U_p were the same, and the second and fourth quadrants showed the results when the polarities were opposite. The electrical tree initiation impulse voltage of the same polarity was much lower than that with a different polarity. In addition, when U_{dc} and U_p were in the same polarity, with the increase of U_{dc} , the initiation impulse voltages decreased for both LI and SI. The change

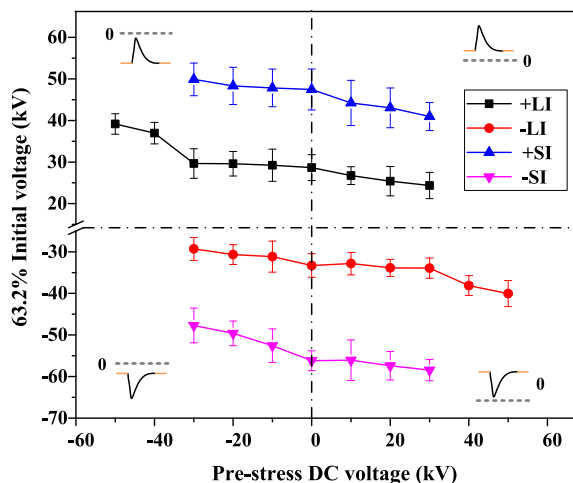


FIGURE 6. Electrical tree initiation properties under DC-impulse composite voltages.

TABLE 2. Electrical tree initiation properties under DC-LI composite voltages.

U_{dc} (kV)	LI initiation voltages (kV)							
	LI(+)	$U_{dc,p}$	SD	CI	LI(-)	$U_{dc,p}$	SD	CI
-50	39.2	-10.8	2.5	0.97	-	-	-	-
-40	37.0	-3.0	2.6	0.99	-	-	-	-
-30	29.7	-0.3	3.7	0.99	-29.3	-59.3	2.8	0.96
-20	29.6	9.6	3.0	0.99	-30.7	-50.7	2.4	0.98
-10	29.2	19.2	3.9	0.98	-31.2	-41.2	3.7	0.97
0	28.7	28.7	3.1	0.98	-33.3	-33.3	2.8	0.98
10	26.7	36.7	2.1	0.98	-32.8	-22.8	2.7	0.97
20	25.4	45.4	3.5	0.99	-33.9	-13.9	2.1	0.99
30	24.4	54.4	3.2	0.97	-33.9	-3.9	2.4	0.98
40	-	-	-	-	-38.1	1.9	2.4	0.97
50	-	-	-	-	-40.0	10.0	3.1	0.97

SD = standard deviation, CI = correlation index.

trend in the paper was the same with that in [17]. When the polarities of U_{dc} and U_p were opposite, the impulse initiation voltages increased with U_{dc} if $|U_{dc}| > 40$ kV; however, there were no significant changes for the impulse initiation voltage when $|U_{dc}| < 40$ kV, which was different from that in [17]. Besides, Fig. 6 also illustrates that the initiation voltages under LI voltage were much smaller than those under SI voltage under all conditions. The trends of initiation properties were the same under DC-LI and DC-SI voltages, despite the initiation voltages under LI being less than those under SI. Therefore, the common initiation properties under DC-LI can somewhat represent the properties under DC-impulse voltages.

Fig. 7 shows a comparison of initiation voltages under DC-LI composite conditions: the 63.2% initiation voltage in the figure represented the absolute value. As can be seen from Fig. 7, there was a notable polarity effect under DC-impulse composite voltages. The electrical tree initiation voltages under positive impulse voltage were smaller than those under negative voltages for both LI and SI, regardless of the polarity of U_{dc} . More specifically, when DC-impulse composite voltages were of the same polarity, the initial voltage with

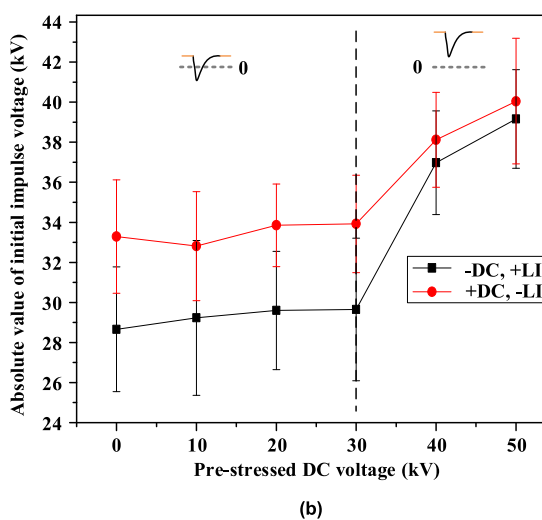
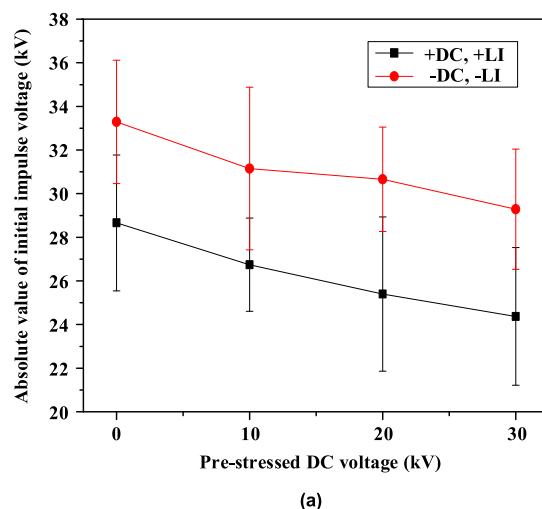


FIGURE 7. Comparison of initial voltages under DC-LI composite voltages in the same, and opposite, polarities. (a) DC-LI in the same polarity. (b) DC-LI in the opposite polarity.

a positive polarity ($U_{+dc,+p}$) was lower than the negative counterparts ($U_{-dc,-p}$). In the presence of opposite polarity, the inception voltage under positive impulse ($U_{-dc,+p}$) was smaller.

During testing, it was found that the length of electrical tree under DC-impulse composite voltages was affected by the amplitude and polarity of the impulse voltage. Fig. 8 shows some representative electrical tree pictures under composite voltages. The length of the initiated electrical tree was relatively long once the electrical tree was initiated, as Fig. 8 showed. Comparing Fig. 8(a) and (b), it was seen that the tree lengths under LI voltages were greater than those under SI voltages when the voltage amplitudes of LI and SI were similar. Fig. 8(c) and (d) revealed that the electrical tree average length with positive impulse voltages was larger than that with negative voltages. Besides, the inception electrical tree length under DC-impulse voltage of the opposite polarity was shorter than that under a pure impulse voltage, as shown in Fig. 8(a) and (c). Furthermore, it was interesting to find that an instant channel breakdown might occur under $U_{+dc,+p}$

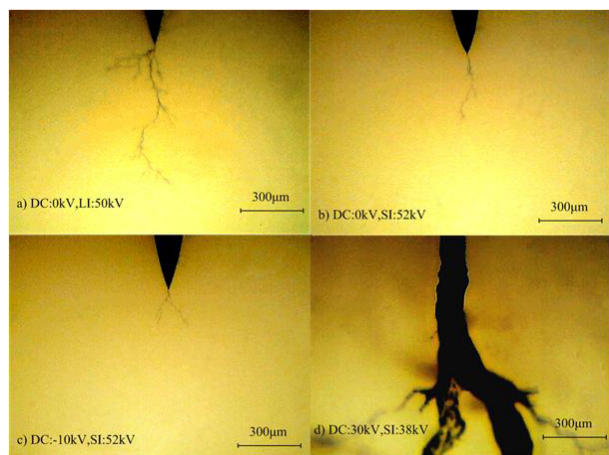


FIGURE 8. Initiation tree pictures under different types of composite voltages.

once the electrical tree initiated, as presented in Fig.8(d). This phenomenon only occurred under $U_{+dc, +p}$, even though the amplitude of $U_{-dc, -p}$ was much greater. This will be discussed in detail in the following section.

IV. DISCUSSION

A. ELECTRICAL TREE INCEPTION UNDER LI AND SI VOLTAGES

Fig.5 shows that the initiation voltages under impulse voltages were much smaller than those under DC voltages. Reference [17] pointed out that the time required for the build-up of space charges near the needle tip was between 30 to 80 μ s. Thus, homo space charges would still form and accumulate near the needle point under an applied impulse voltage. Compared to DC conditions, the transient peak value of the impulse voltage could rise 30% to 50% in a much shorter time. Therefore, fewer homo space charges accumulated near the needle point, and the electrical field strength would be much larger than that under DC voltage. Hence, the impulse initiation voltage was much lower than that under the applied pure DC voltage. Generally, a solid dielectric is more sensitive to the impulse voltage with a steeper edge, due to its steep electrical field gradient. Compared to a SI voltage, LI has a much steeper rising edge with a much larger electrical field gradient. Besides, the shorter rise time would lead to less space charge accumulation and a smaller initiation voltage. That may be the reason why the initiation voltage under LI was smaller than that under SI.

B. TREE INCEPTION UNDER DC-IMPULSE COMPOSITE VOLTAGES OF THE SAME POLARITY

For tests under DC-impulse composite voltages, a pre-stressed DC voltage was first applied to the samples. The DC voltage was increased at a rate of 1 kV/s and held for 10 s. There would be enough time for the injected space charges to form a steady distribution. The electron traps distribution properties in epoxy resin under DC-impulse voltage with the same polarity was investigated in [24], and it pointed

out that with the increasing of pre-stressed DC voltage, the electron trap density increased. And the electron trap density was much larger than that under impulse voltage. Once the trapped space charges were stimulated by external factors, such as high electrical field, mechanical stress, abrupt temperature change, radiation, etc., a significant amount of electrical-mechanical energy caused by the extraction or recombination of space charges would be released instantaneously and cause the cleavage of polyethylene molecular chains. Therefore, the more space charge accumulated, the larger electrical-mechanical energy would release, which would cause electrical tree initiation more easily.

As Fig.6 and Fig.7(a) show, under DC superimposed impulse voltage of the same polarity, the initiation voltages decreased with U_{dc} increasing. Existing research [21] shows that the electrical field around the needle tip thereupon increased. The enhanced electric field would thus promote more high-energy space charges to de-trap and cause intense partial discharge. Immense electromechanical and thermal energy would be released by the de-trapping and recombination of space charges, which would make it easier for tree initiation. So, with the increase of the pre-stressed DC voltage, the initiation impulse voltages decreased gradually, as shown in Fig.6 and Fig.7(a).

C. TREE INCEPTION UNDER DC-IMPULSE COMPOSITE VOLTAGES OF OPPOSITE POLARITY

The initiation characteristics under DC-impulse composite voltages of the opposite polarity differed (Fig.6 and Fig.7(b)). For tests under DC-impulse composite voltages of the opposite polarity, a pre-stressed DC voltage (such as a -DC) was first applied to the samples and the space charges would accumulate around the needle tip. When an impulse voltage of the opposite polarity (such as a +impulse) was applied to the sample, the electrical field near the needle tip would drop abruptly, and the trapped space charges would form a reverse field which pointed to the needle. Afterwards, the massive trapped charges would de-trap from the XLPE electron traps. The changes in electrical field distribution and the dynamic property of space charges around needle tip were similar to those of a grounded DC tree [14] (the so-called “grounded effect”). Besides, during the falling edge of the impulse voltage, the voltage would return to the pre-stressed DC voltage in a relatively short time and the space charges would also be re-injected into the sample. The re-injection of space charges would also facilitate the initiation of electrical trees [6]. The de-trapping and re-injection process would cause the fracture of XLPE molecular chains and result in the initiation of electrical trees when the impulse voltage was high enough. This process might be the main factor determining electrical tree initiation.

As shown in Fig.7(b), when $|U_{dc}| < 40$ kV, the initiation impulse voltages did not change. For this stage, it could be found that the amplitude of initiation impulse voltage was greater than the pre-stressed DC voltage ($|U_p| > |U_{dc}|$), thus there would be a stage in which the polarity reversed

for the DC-impulse composite voltages. In this situation, except for the de-trapping and re-injection process described above, recombination of space charges would also occur during polarity reversal of DC-impulse voltages. The energy released by the recombination would also promote the initiation of electrical trees. That is why the electrical trees were more likely to be initiated during polarity reversal [15], [25]; however, it should be noted that the electrical tree initiation voltage did not change to any significant extent even if the pre-stressed DC amplitude increased in the first stage (the recombination process would decrease with U_{dc} increasing). This may reveal that the recombination process played a supplementary, but non-negligible role in the inception of electrical trees. The inception of electrical trees at this stage was mainly determined by the grounded effect.

When the DC voltages exceeded 40 kV, the initiation voltages also increased and the initiation impulse voltages were much greater than those when $|U_{dc}| < 40$ kV (Fig.7(b)). In this stage, the absolute value of the impulse voltage was less than the pre-stressed DC voltage ($|U_p| < |U_{dc}|$), namely the DC-impulse voltages would never exceed zero ($|U_{dc,p}| > 0$). At this time, the change in the electrical field distribution around needle tip was similar to that of a grounded DC tree. The inception properties could be explained by the de-trapping and re-injection process described above. With the increase of pre-stressed DC voltage, the total DC-impulse voltage increased and there would be more space charge retaining near the needle tip, thus increasing the homogenisation effect and increasing the inception voltage. This might be why the initiation impulse voltage increased.

D. POLARITY EFFECT ON ELECTRICAL TREE INITIATION UNDER DC-IMPULSE VOLTAGES

The polarity effect on the electrical tree initiation under DC-impulse composite voltages was shown in Fig.7(a) and (b). When DC and impulse voltages were of the same polarity, the initial voltage with positive polarity was less than that with the negative counterpart; however, in the case of the opposite polarity, the inception voltage under $U_{-dc,+p}$ was lower.

As for the case of DC-impulse voltages of the same polarity, when DC-impulse voltages were applied to the sample, electrons or holes would be injected into the insulation, depending on the polarity of the pre-stressed DC voltage. Compared to holes, electrons occupied a smaller volume and had a larger mean free path, resulting in a larger space charge layer, which would weaken the electrical field near the needle tip, and a large impulse voltage was needed for initiation of electrical trees. That is why the initiation impulse voltage under $U_{-dc,-p}$ was larger than that under $U_{+dc,+p}$.

Nevertheless, as for the condition of DC-impulse voltages of the opposite polarity, the extensively accumulated electrons would play a favourable role in the initiation of electrical trees. The anti-electrical field, formed by the injected space charges when the impulse voltage applied, would be

stronger under $U_{-dc,+p}$. Furthermore, the de-trapping and re-injection process would be more intense during the falling edge. Thus, electrical trees were more likely to be initiated under $U_{-dc,+p}$.

E. ELECTRICAL TREE BREAKDOWN UNDER POSITIVE DC-IMPULSE VOLTAGES

During testing, with DC voltage amplitude increasing, the possibility of instantaneous channel breakdown from needle tip to grounded electrode increased under $U_{+dc,+p}$, as shown in Fig.8(d); however, there were no occurrences thereof under negative conditions, even though the amplitude of $U_{-dc,-p}$ was much larger. A similar phenomenon was also found in previous researches [26]–[28]. Electron avalanche theory was used to explain the breakdown and electrical tree degradation in polymer [28], [29], which might explain the aforementioned phenomenon. The formation of the electron avalanche in the solid was similar to that in gas. The obtained kinetic energy (KE) of the accelerated electron was determined by the free-path length (λ) in solid, and both KE and λ were treated as adjustable parameters. As [29] described, the kinetic energy and free-path length could be taken as 9.6eV and ~ 60 nm for polyesters, respectively. The energy was larger than the bond energy in XLPE (C-C, ~ 3.44 eV; C-H, ~ 4.29 eV), and it would fracture and ionize the molecule chains. The process would carry on in the form of a chain reaction and an avalanche would form. Once an electron avalanche formed, it would be directed towards the needle point under the influence of the electrical field created by $U_{+dc,+p}$, leaving behind a wedge-shaped region of holes. The wedge-shape avalanche would strengthen the electrical field ahead of its leading edge, thus forming a sequence of avalanches and channel erosion. At this time, the positive streamer discharge formed and developed forward to the grounded electrode. Once the further tip of electrical tree channel reached the grounded electrode, a short circuit would occur. This process may stop when the electrons produced can no longer acquire sufficient KE to ionize the molecule, resulting in the extinction of the electron avalanche and the stopping of electrical tree growth.

V. CONCLUSION

Experiments were performed to study the electrical tree initiation properties in XLPE under DC-impulse composite voltages. The influence of pre-stressed DC voltage, impulse voltage, polarity and space charge accumulation on the initiation characteristics were investigated and analysed. The following conclusions could be drawn.

1) The wave-front time of the impulse voltage influenced the initiation characteristics of electrical tree under impulse voltage and DC-impulse voltage. The electrical tree initiation voltages under DC-LI were smaller than those under DC-SI composite voltages, due to its steeper wave-front.

2) The electrical tree initiation impulse voltage of the same polarity was much smaller than those of the opposite polarity. With DC voltage increasing, the initiation impulse voltage

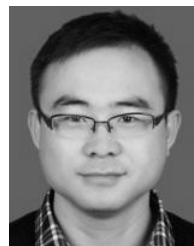
decreased for samples of the same polarity; however, for those samples of the opposite polarity, there were no obvious changes when $|U_{dc}| < |U_p|$, and the initiation impulse voltage increased when $|U_{dc}| > |U_p|$.

3) A polarity effect was observed under DC-impulse composite voltages clearly. The electrical tree initiation voltages under positive impulse voltage were smaller than those under negative voltages.

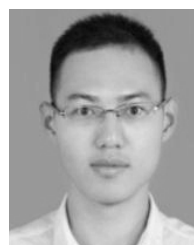
4) When the DC cable is subjected to a sudden impulse voltage during operation, an electrical tree may be initiated if there is a pre-existing defect. And the electrical tree is more likely to initiate if the DC cable is subjected to a positive impulse voltage.

REFERENCES

- [1] R. Schurch, P. Donoso, P. Aguirre, O. Cardenas, M. Zuniga, and S. M. Rowland, "Electrical tree growth and partial discharges analyzed by fractal and correlation dimensions," in *Proc. IEEE Conf. Electr. Insul. Dielectric Phenomenon (CEIDP)*, Ft Worth, TX, USA, Oct. 2018, pp. 785–788.
- [2] B. X. Du, J. G. Su, and T. Han, "Compressive stress dependence of electrical tree growth characteristics in EPDM," *IEEE Trans. Dielectrics Electr. Insul.*, vol. 25, no. 1, pp. 13–20, Feb. 2018.
- [3] Y. Liu, Y. Li, H. Liu, X. Zheng, and M. Fu, "Research of grounded DC tree growth characters and propagation structure in XLPE," (in Chinese), *High Voltage Eng.*, vol. 43, no. 11, pp. 3551–3558, Nov. 2017.
- [4] C. Zhuang, Y. Zhang, X. Zhou, R. Zeng, J. He, and L. Liu, "A fast tree algorithm for electric field calculation in electrical discharge simulations," *IEEE Trans. Magn.*, vol. 54, no. 3, Mar. 2018, Art. no. 7201304.
- [5] Y. Zhang, Y. Zhou, L. Zhang, Z. Lin, J. Liu, and Z. Zhou, "Electrical treeing behaviors in silicone rubber under an impulse voltage considering high temperature," *Plasma Sci. Technol.*, vol. 20, no. 5, p. 054012, Apr. 2018.
- [6] Y. Liu and X. Cao, "Electrical tree growth characteristics in XLPE cable insulation under DC voltage conditions," *IEEE Trans. Dielectrics Electr. Insul.*, vol. 22, no. 6, pp. 3676–3684, Dec. 2015.
- [7] Y. Wang, F. Guo, J. Wu, and Y. Yin, "Effect of DC prestressing on periodic grounded dc tree in cross-linked polyethylene at different temperatures," *IEEE Access*, vol. 5, pp. 25876–25884, 2017.
- [8] L. K. H. Pallon *et al.*, "Three-dimensional nanometer features of direct current electrical trees in low-density polyethylene," *Nano Lett.*, vol. 17, no. 3, pp. 1402–1408, Feb. 2017.
- [9] M. Ieda and M. Nawata, "DC treeing breakdown associated with space charge formation in polyethylene," *IEEE Trans. Electr. Insul.*, vol. EI-12, no. 1, pp. 19–25, Feb. 1977.
- [10] Y. Sekii, H. Kawanami, M. Saito, K. Sugi, and I. Komatsu, "DC tree and grounded DC tree in XLPE," in *Proc. Conf. Electr. Insul. Dielectric Phenomena (CEIDP)*, Nashville, TN, USA, Oct. 2005, pp. 523–526.
- [11] I. Kitani and K. Arii, "DC tree associated with space charge in PMMA," *IEEE Trans. Electr. Insul.*, vol. EI-22, no. 3, pp. 303–307, Jun. 1987.
- [12] B. X. Du, J. G. Su, and T. Han, "Effects of mechanical stretching on electrical treeing characteristics in EPDM," *IEEE Trans. Dielectrics Electr. Insul.*, vol. 25, no. 1, pp. 84–93, Feb. 2018.
- [13] Y. Zhang, L. Zhang, Y. Zhou, M. Chen, M. Huang, and R. Liu, "Temperature dependence of DC electrical tree initiation in silicone rubber considering defect type and polarity," *IEEE Trans. Dielectrics Electr. Insul.*, vol. 24, no. 5, pp. 2694–2702, Oct. 2017.
- [14] Y. Liu, H. Liu, Z. Yang, Y. Li, L. Yu, and H. Rui, "Effect of DC pre-stress on the initiation characteristics of grounded DC tree in XLPE," (in Chinese), *High Voltage Eng.*, vol. 43, no. 2, pp. 666–672, Feb. 2017.
- [15] Y. Zhang, Y. Zhou, M. Chen, L. Zhang, X. Zhang, and Y. Sha, "Electrical tree initiation in silicone rubber under DC and polarity reversal voltages," *J. Electrostatics*, vol. 88, pp. 207–213, Jan. 2017.
- [16] B. X. Du, M. M. Zhang, J. X. Jin, and Y. Xin, "Tree growth characteristics of epoxy resin in LN₂ under magnetic field," *IEEE Trans. Appl. Supercond.*, vol. 26, no. 3, Apr. 2016, Art. no. 7700705.
- [17] F. Noto, N. Yoshimura, and T. Ohta, "Tree initiation in polyethylene by application of DC and impulse voltage," *IEEE Trans. Electr. Insul.*, vols. EI-12, no. 1, pp. 26–30, Feb. 1977.
- [18] S. Fujita, M. Baba, and F. Noto, "Study on breakdown voltage of cylindrical tubule and tree growth in PMMA," in *Proc. Int. Symp. High Voltage Eng.*, Graz, Austria, 1995.
- [19] L. Ying and C. Xiaolong, "Electrical tree initiation in XLPE cable insulation by application of DC and impulse voltage," *IEEE Trans. Dielectrics Electr. Insul.*, vol. 20, no. 5, pp. 1691–1698, Oct. 2013.
- [20] X. Chen *et al.*, "AC and DC pre-stressed electrical trees in LDPE and its aluminum oxide nanocomposites," *IEEE Trans. Dielectrics Electr. Insul.*, vol. 23, no. 3, pp. 1506–1514, Jun. 2016.
- [21] T. Han, B. Du, and J. Su, "Electrical tree initiation and growth in silicone rubber under combined DC-pulse voltage," *Energies*, vol. 11, no. 4, p. 764, Mar. 2018.
- [22] Y. Liu, H. Liu, Y. Li, L. Yu, and H. Rui, "Research of the electrical tree properties in XLPE under DC-AC composite voltages," (in Chinese), *Trans. China Electrotechnical Soc.*, vol. 33, no. 03, pp. 601–608, Feb. 2018.
- [23] B. X. Du, J. G. Su, and J. S. Xue, "Tree Growth characteristics of epoxy resin in LN₂ under DC superimposed pulse voltage," *IEEE Trans. Appl. Supercond.*, vol. 28, no. 4, Jun. 2018, Art. no. 7700105.
- [24] M. Abou-Dakka, A. Bulinski, and S. S. Bamji, "Effect of additives on the performance of cross-linked polyethylene subjected to long term single and periodically reversed polarity DC voltage," *IEEE Trans. Dielectrics Electr. Insul.*, vol. 20, no. 2, pp. 654–663, Apr. 2013.
- [25] H. Liu, Y. Liu, Y. Li, P. Zheng, and H. Rui, "Growth and partial discharge characteristics of electrical tree in XLPE under AC-DC composite voltage," *IEEE Trans. Dielectrics Electr. Insul.*, vol. 24, no. 4, pp. 2282–2290, Aug. 2017.
- [26] I. Idrissu, H. Zheng, and S. M. Rowland, "DC electrical tree growth in epoxy resin and the influence of the size of inceptive AC trees," *IEEE Trans. Dielectrics Electr. Insul.*, vol. 24, no. 3, pp. 1965–1972, Jun. 2017.
- [27] I. Idrissu, H. Zheng, S. M. Rowland, "Electrical tree growth in epoxy resin under DC voltages," in *Proc. IEEE Int. Conf. Dielectrics (ICD)*, Piscataway, NJ, USA, Jul. 2016, pp. 820–823.
- [28] L. A. Dissado and P. J. J. Sweeney, "Physical model for breakdown structures in solid dielectrics," *Phys. Rev. B, Condens. Matter*, vol. 48, no. 22, pp. 16261–16268, Dec. 1993.
- [29] I. Kitani and K. Arii, "Impulse tree and discharge light in Pmma subjected to nanosecond pulses," *IEEE Trans. Electr. Insul.*, vols. EI-19, no. 4, pp. 281–287, Aug. 1984.



HECHEN LIU was born in Hengshui, Hebei, China, in 1989. He received the B.Eng. and Ph.D. degrees in electrical engineering from North China Electric Power University, Baoding, China, in 2012 and 2017, respectively. He is currently a Lecturer with North China Electric Power University. His research interests include the insulation monitoring of power cable and ageing mechanisms in high-voltage apparatus.



YANDA LI was born in Jilin City, Jilin, China, in 1993. He received the B.Eng. degree in electrical engineering from North China Electric Power University, Baoding, China, in 2016, where he is currently pursuing the M.Eng. degree with the School of Electrical Engineering. His research interests focus on the space charge characteristics of HVDC cables.



YUNPENG LIU was born in Jinzhai, Anhui, China, in 1976. He received the B.Eng. and Ph.D. degrees in electrical engineering from North China Electric Power University, Baoding, China, in 1999 and 2005, respectively. He is currently a Ph.D. Supervisor and a Professor with North China Electric Power University. His research interests include UHV transmission, and fault detection and diagnosis in electrical and electronic equipment.



XIAOBIN XU was born in Handan, Hebei, China, in 1995. She received the B.Eng. degree in electrical engineering from North China Electric Power University, Baoding, China, in 2018, where she is currently pursuing the M.Eng. degree with the School of Electrical Engineering. Her research interests mainly focus on the electric field and space charge distribution in HVDC cable insulation.



MINGJIA ZHANG was born in Taizhou, Zhejiang, China, in 1995. He received the B.Eng. degree in civil engineering from Northeast Electric Power University, Jilin, China, in 2017. He is currently pursuing the M.Eng. degree with North China Electric Power University. His research interests focus on the aging characteristics of the HVDC cables and composite cross-arms.



AIJING LIU was born in Chaoyang, Liaoning, China, in 1995. She received the B.Eng. degree in electrical engineering from North China Electric Power University, Baoding, China, in 2018, where she is currently pursuing the M.Eng. degree with the School of Electrical Engineering. Her research interests focus on the temperature field distribution characteristics of ac and dc cables.

...